MNRAS 000, 1–?? (2016) Preprint September 28, 2017 Compiled using MNRAS LaTeX style file v3.0

Dynamics in primordial black hole clusters

Valeriya Korol[1,2⋆], Ross P. Church[2,3], Melvyn B. Davies[2,3], Ilya Mandel[2,4] and M. Coleman Miller[2,5]

[1] *Leiden Observatory, Leiden University, PO Box 9513, 2300 RA, Leiden, the Netherlands*
[2] *DARK, Niels Bohr Institute, University of Copenhagen, Blegdamsvej 17, 2100 Copenhagen, Denmark*
[3] *Lund Observatory, Department of Astronomy & Theoretical Physics, Lund University, Box 43, SE-221 00 Lund, Sweden*
[4] *School of Physics and Astronomy, University of Birmingham, Edgbaston, Birmingham B15 2TT, United Kingdom*
[5] *Department of Astronomy, University of Maryland, College Park, MD 20742-2421, USA*

September 30, 2017

ABSTRACT

This is a draft version of the paper based on the summer project developed during the Kavli Summer Program in Astrophysics 2017 by Valeriya Korol and co-authors at Niels Bohr Institute (Copenhagen). Following the theme of 2017 *Astrophysics with gravitational wave detections* we worked on few-body dynamical simulations and their application to Gravitational Wave Astrophysics.

In this project we found many interesting results concerning the estimation of black hole (BH) binaries merger rates. Our results indicate that the estimates for the merger rate of binary BHs of primordial origin, made by several authors after the first detection of gravitational waves by the Advanced LIGO, should be conducted more carefully. In particular, we suggest that few-body dynamical interactions may play an important role in the regime that mostly contributes to the total merger rate of primordial BH binaries. However, more simulations are required before presenting our final results on the merger rate of primordial BHs in the regime we explore. The results presented in this draft should be considered preliminary.

Key words: stellar dynamics, primordial black holes, gravitational waves

1 INTRODUCTION

The concept of black holes formed directly from gravitational collapse of the cosmological density fluctuations in the early Universe, that for this reason are called primordial, dates back to 1970s (Hawking 1971). Once collapsed primordial black holes (PBHs) would then behave as non-baryonic cold dark matter (DM) throughout the subsequent evolution of the Universe. The large variety of mechanisms that could have produce PBHs gives a mass function that extends from the Planck mass to $10^{15}\,\mathrm{M}_\odot$ (see Carr et al. 2016, for a review). Depending on the mass, their abundance could comprise the total content of DM in the Universe. However, different astrophysical and cosmological experiments have placed strong limits on the abundance of PBHs, leaving three mass windows in which PBHs can still provide an important contribution to the DM content: asteroid mass PBHs ($10^{16} - 10^{17}$ g), sub-lunar mass PBHs ($10^{20} - 10^{26}$ g) and PBHs of $20 - 100\,\mathrm{M}_\odot$ (Carr et al. 2016).

Recently, the detection of gravitational waves (GWs) from merging BH binaries by the Advanced LIGO (Laser Interferometer Gravitational-Wave Observatory) offered a possibility to interpret these events as the coalescence of PBH binaries (Abbott et al. 2016; Bird et al. 2016; Clesse & García-Bellido 2016; Sasaki et al. 2016; Ali-Haïmoud et al. 2017). In particular, three of the events involved mergers of BHs with masses estimated to be near $30\,\mathrm{M}_\odot$, that falls into the mass window between 20 and 100 $\mathrm{M}_\odot$, where PBH could largely contribute to the content of DM. The strongest constraints in this mass regime come from microlensing observation of stars in the Large and Small Magellanic Clouds at the low mass end (Paczynski 1986; Alcock et al. 2000; Tisserand et al. 2007), and from observations of wide binaries in the Milky Way halo at the high mass end (Yoo et al. 2004; Quinn et al. 2009). It is noteworthy that the limits from cosmic microwave background observations can completely rule out the existence of PHBs in this mass range. However, considering that the limits are model dependent and based on uncertain physical parameters, their validity is still under debate.

In the scenario in which all DM consists of $30\,\mathrm{M}_\odot$ PBHs, it has been shown that the formation of PBH binaries by

⋆ E-mail:korol@strw.leidenuniv.nl

the gravitational two-body capture mechanism in DM halos can give a merger rate comparable to the merger rate inferred from LIGO detections (Bird et al. 2016; Clesse & García-Bellido 2016; Ali-Haïmoud et al. 2017). In contrast with previous works, in this paper we explore regimes where dynamics of the DM halo is dominated by three-body encounters. In this case we find that the first hard binary is formed within ~ 10 crossing times. We show that after the formation of the first binary the subsequent evolution of the PBH cluster is completely dominated by the hard binary, that leads to evaporation of the cluster in 30 crossing times.

This paper is organized as follows. In Section 2 we briefly review results from Bird et al. (2016) and describe the setup for our simulations. In Section 3 we present the obtained results. In Section 4 we estimate the merger rate in our simulations. Finally, in Section 4 we discuss the implications of our results for PBH merger rate.

2 SIMULATION SETUP

To the set up our simulation we use the results from Bird et al. (2016). We assume that all PBHs have a single mass of $30\,M\odot$, and that their large scale distribution follows that of DM halos. There is a finite probability that within a halo two initially unbound PBHs pass close enough to each other to produce GW emission. If the energy released in GWs at the closest passage exceeds the sum of initial kinetic energies, the BH pair becomes gravitationally bound. This, so-called gravitational two-body capture mechanism, typically forms very tight and eccentric binaries, so that the binary coalescence time is much shorter than a Hubble time (Cholis et al. 2016). Thus, the merger rate is approximately equal to the binary formation rate and is of the order of $10^{-2}\,\mathrm{Gpc}^{-3}\mathrm{yr}^{-1}$, depending on the choice for the DM halo mass function and the cutoff mass. In particular, the major contribution to the merger rate of PBH binaries would come from small DM halos (see Figure 2 of Bird et al. 2016). This is a consequence of two effects. First, the velocity dispersion in small mass halos is lower ($\sigma_\mathrm{v} \propto \sqrt{M}$, where M is the mass of the halo), and thus the energy that needs to be irradiated in GWs to bind the PBH pair is smaller. Second, small halos are more concentrated, thus the number of mergers per halo ($N \propto n$, where n is the number density of PBH in the halo) is higher. Thus, in our work we will consider halos of $\sim 10^3\,M\odot$ or smaller. Note, a halo of $10^3\,M\odot$ would consist of a few objects only. In a few-body regime the timescale arguments are no longer accurate and direct simulations are required to predict the outcome for the dynamical evolution of the system.

For this work we model three fiducial clusters:

(i) $15 \times 30\,M\odot$ PBHs,
(ii) $5 \times 30 + 30 \times 10\,M\odot$ PBHs,
(iii) $35 \times 30\,M\odot$ PBHs,

such that the first two have the same total mass ($450\,M\odot$), while the second and the third ones have the same number of objects (35). We set the size of the cluster to be $R = 1\,\mathrm{pc}$. We draw the initial positions of PBHs from a uniform space-density distribution and velocities from a Maxwellian distribution with the scale parameter equal to $\sigma_\mathrm{v} \sim \sqrt{GM/R}$, where G is the the Gravitational constant. To make our stimulations scale-free, we fix the virial ratio (ratio of kinetic to potential energy) of the cluster to $0.5, 0.3$ and 0.1. Note, that these clusters are more compact compared to Bird et al. (2016), so that in our simulations PBH binaries can form through non-dissipative three-body interaction. In three-body encounters one PBH removes enough kinetic energy to leave the other two in a bound state. Because our simulations are scale-free, we can rescale the obtained results to compare with those from Bird et al. (2016).

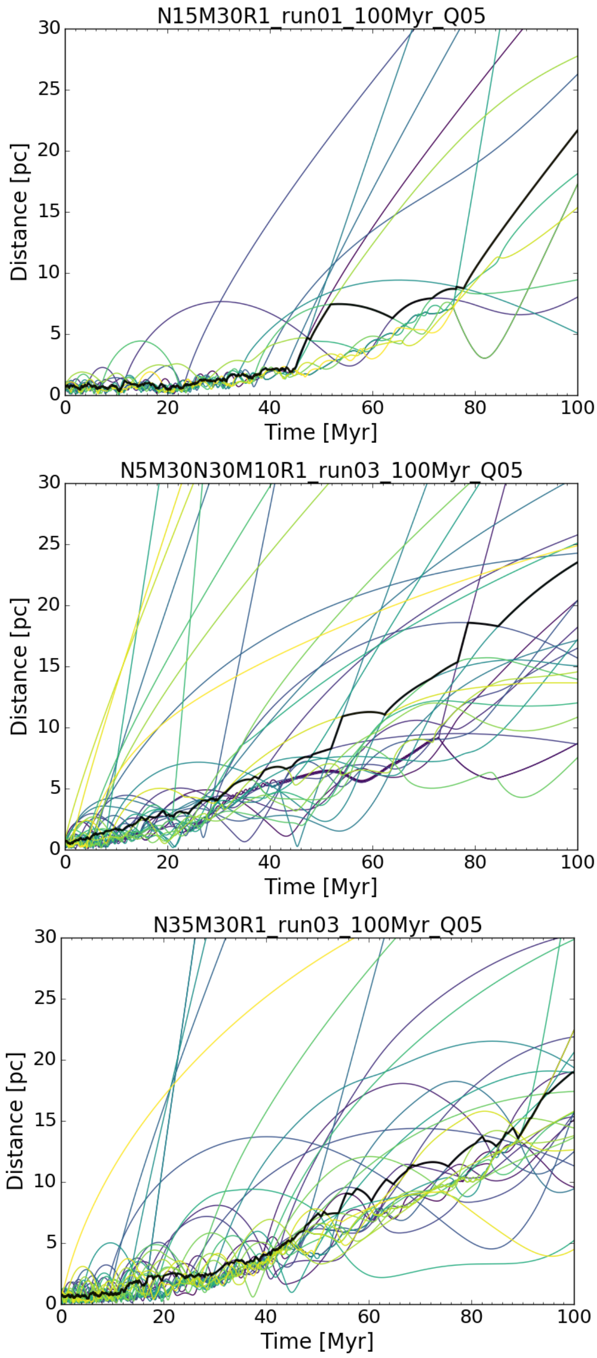

Figure 1. Distance from the barycenter as a function of time: each line represents one PBH. From the top to the bottom for cluster (i),(ii) and (iii). The black solid line represents the median distance.

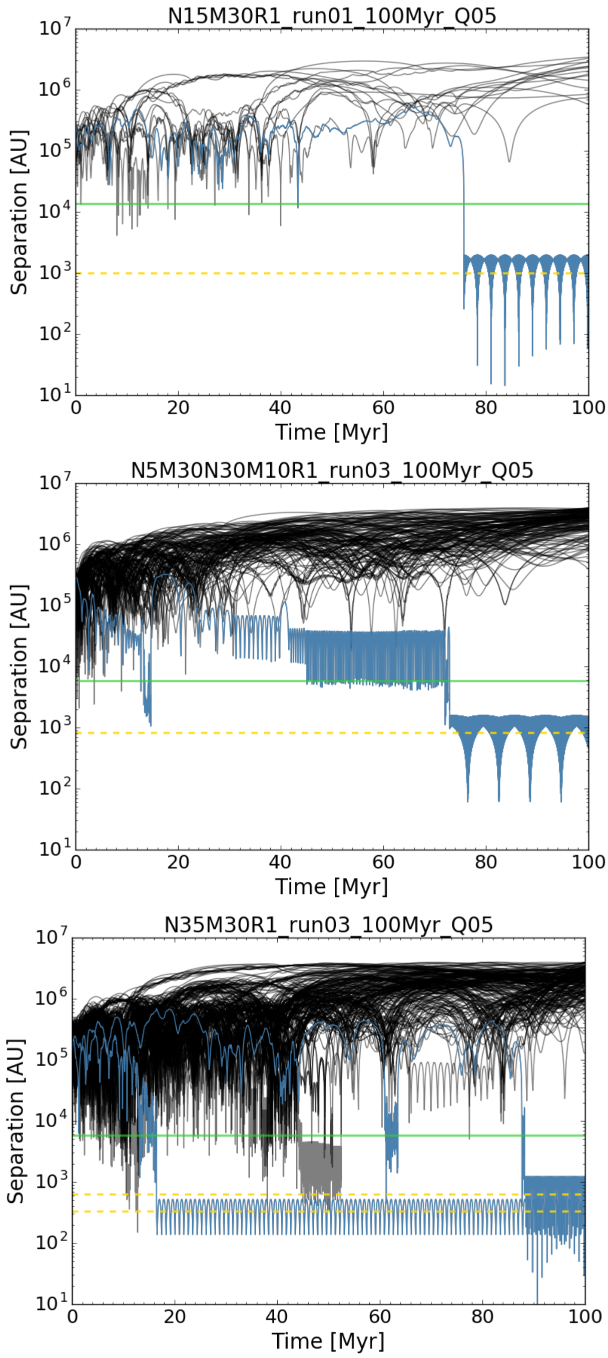

Figure 2. Separation between two PBHs as a function of time: each line represent a pair of PBHs. From the top to the bottom for cluster (i), (ii) and (iii). In blue we color PBH pairs that become bound. The green solid line shows the separation between hard and soft binaries. Yellow dashed lines represent the semi-major axis of the formed binaries.

To simulate the dynamical evolution of these clusters we use REBOUND, an N-body open source code with an IAS15 integrator (Rein & Liu 2012; Rein & Spiegel 2015). We performed 60 simulations in total: 10 for each type of cluster and for each value of the virial ratios. We let our PBH clusters evolve for 100 Myr under the influence of gravity only. This corresponds to 200 $t_{\rm cross}$, where $t_{\rm cross} = R/\sigma_{\rm v}$, for 450 M⊙ clusters and to $\sim 80\, t_{\rm cross}$ for 1050 M⊙ clusters. No additional forces or effects, like general relativity or tidal forces, are considered.

3 RESULTS

During our simulations we trace the formation of PBH binaries, their properties, and to how many other PBHs they are bound. In this section, first, we show some representative examples of the simulation runs for each type of cluster, then we summarize the result for the whole set of simulations.

We find that at the end of the simulations the clusters are very spread-out with an average distance from the center of mass that is more that an order of magnitude higher compare to initial size of the cluster. Figure 1 shows the distance of PBHs from the barycenter of the cluster as a function of time (each line represents a single PBH): from the top to the bottom for the cluster i), ii) and iii). One can see that the majority of the lines intertwine for the first half of the simulation indicating that the cluster stays bound. Arched lines represent objects that are kicked out of the cluster with velocities lower than the escape velocity, such that they fall back into the cluster after reaching a maximum distance. Vertical lines indicate PBH that are ejected from the cluster. We do not remove ejected objects ans as a consequence the average distance of those PBHs that are bound drifts from 0, as it is clearly visible in Fig. 1. Finally, from the bottom to the top panel one can see that the clusters break up faster.

In Fig. 2 we plot the separation between every pair of PBHs in the cluster, i.e. $|\mathbf{r}_{\rm i} - \mathbf{r}_{\rm j}|$ where $\mathbf{r}$ is the position vector of the object in the cluster's barycenter reference frame. To not over complicate the plot we represent only those pairs whose separation at the end of the simulation is less than 10 pc. In blue we colour those pairs that form a binary. The green solid line represents the separation between hard and soft binaries ($a_{\rm HS} \sim R/N$, where N in the total number of PBHs in the cluster). The yellow dashed line indicates the semi-major axis of the binary at $t = 100$ Myr. These examples illustrate that the typical outcome of our simulations is the formation of one or two hard binaries, while the rest of the PBHs have separations much larger than the original size of the cluster. The different number of lines clearly illustrates that clusters of type ii) and iii) stay compact during for longer time, and require more time to evaporate.

It is well known that binaries are the energy source in a cluster. The heating of the clusters by the dynamical interaction of binaries and field stars can cause it to heat up, expand and in some cases even evaporate. To determine whether this is also the case in our simulations we trace the formation time of the first hard binary. Besides, we arbitrarily define the evaporation time of the cluster as the time when the median separation between PBHs is twice the initial size of the cluster. We find that for the majority of the clusters the first hard binary is formed within 10 $t_{\rm cross}$ and that the cluster evaporates in $\sim 30\, t_{\rm cross}$. This indicates that hard binaries heat the cluster through encounters with single PBHs. In this paragraph calculations (or plots) are necessary to prove this concept.

Finally, we summarize the properties of all the hard binaries formed in our simulations in Fig. 4 by showing their

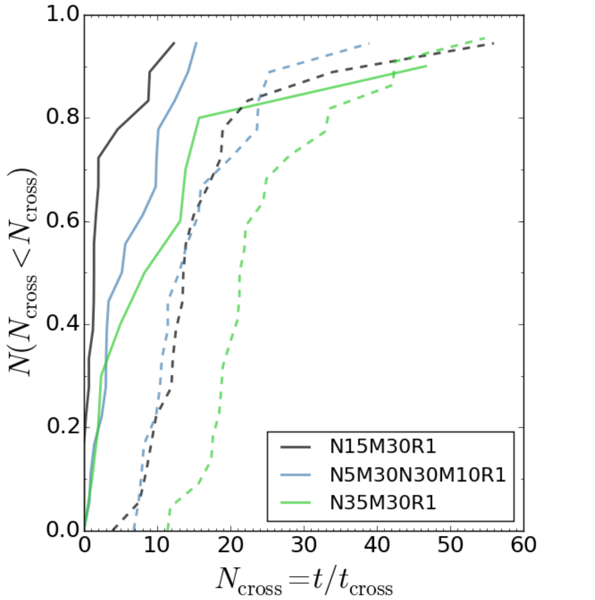

Figure 3. Cumulative distribution of the time of formation of the first hard binary (solid lines) and the cluster evaporation time (dashed lines) as a function of the number of crossing times. We define the cluster evaporation time as the time when the median separation between PBHs is twice the initial size of the cluster. The legend can be interpreted as follows: N stands for the number of objects, M is the PBH mass and R is the size of the cluster.

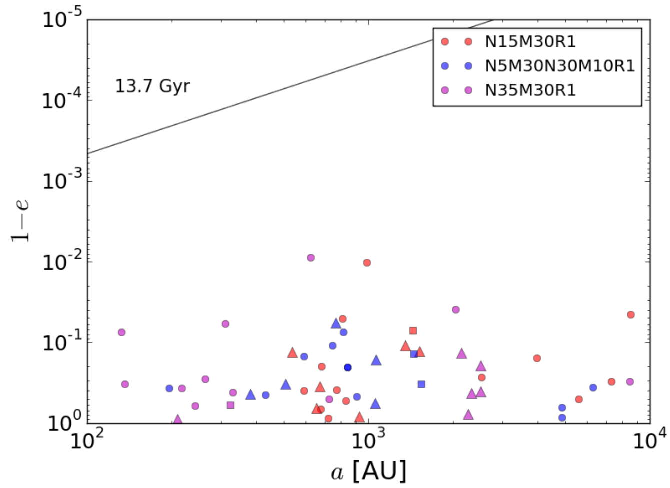

Figure 4. Properties of the binaries formed in our simulations: circles are binaries that are not bound to any other PHB, triangles are triples and squares are multiple systems. The black solid line iso-merger line for a $30 + 30\,\mathrm{M}\odot$ PBH binary. The legend can be interpreted as in Fig.3.

eccentricity (in terms of $1-e$) and the their semi-major axes: circles are binaries that are not bound to any other PHB, triangles are triples and squares are multiple systems. It is easy to see that in our simulations we mainly form binaries that are not bound to other PBHs, rarely we form triples, and, only in a few cases we have multiple systems. We find that the distribution of binary semi-major axes rages from 10^2 to 10^4 AU. We verify that the eccentricity distribution follows the thermal distribution.

For a circular binary with semi-major axis a, the time it takes it to merge due to GW radiation is given by (Peters 1964):

$$T_{\rm GW,0} \approx 6{\times}10^{11}\,{\rm yr} \left(\frac{a}{100\,{\rm AU}}\right) \left(\frac{\mu}{15\,{\rm M}\odot},\right)^{-1} \left(\frac{m_1+m_2}{60\,{\rm M}\odot}\right)^{-2} \tag{1}$$

while for a highly eccentric binary with initial eccentricity e

$$T_{\rm GW}(a,e) \approx \frac{768}{425}(1-e^2)^{7/2}\; T_{\rm GW,0}, \tag{2}$$

where $\mu = m_1 m_2/(m_1+m_2)$ is the reduced mass of the binary and $m_{1,2}$ are masses of the binary components. Equation (1) shows that circular binaries formed in our simulation need more than the age of the Universe to merge due to GW emission. However, for PBH binaries with $e \sim 1$, the merger time reduced reduces significantly (eq.(2)). The black solid line in Fig.4 is obtained by numerically integrating Eq.(5.7) of Peters (1964), and represents the coalescence time of 13.7 Gyr for a $30+30\,\mathrm{M}\odot$ PBH binary. It clearly shows that even for the most tight binaries formed in our fiducial clusters $1-e$ should be as small as 10^{-4} (i.e. $e = 0.9999$). Therefore, to produce binaries that will merge in a Hubble time, a mechanism that can induce extremely high eccentricities is required.

4 MERGER RATE FROM THE ECCENTRIC KOZAI-LIDOV MECCANISM

Several authors have pointed out that hierarchical triple systems may undergo large amplitude eccentricity oscillations due to the Eccentric Kozai-Lidov (EKL) mechanism (see Naoz 2016, and references therein). In the ordinary Kozai-Lidov (KL) mechanism the exchange of the angular momentum between inner and outer orbits leads to eccentricity and orientation oscillations (Kozai 1962; Lidov 1962). When the system begins in a configuration such that the inner and the other orbit are highly inclined with respect to each other, the inner orbit eccentricity can rapidly reach extreme values leading to a short orbital period binary or even to the direct merger of the inner binary components. In this Section we estimate how often the condition for the EKL can occur in our simulations. This allows us to infer the merger rate due to EKL effect.

In this section we adopt the following notation: with the index 1 and 2 we will refer respectively to the inner and outer binary. In Fig. 5 we illustrate properties of the triple systems formed in our simulations: circles represent the semi-major axis of the inner and outer binary respectively on the x and y-axis, the error bars on the y-axis represent $a_2(1-e_2)$ and $a_2(1+e_2)$, and the dashed lines are those of a constant ratio a_2/a_1 .

We test the stability of our systems using the criteria from Mardling & Aarseth (2001):

$$\frac{a_2}{a_1} < 2.8\left(1+\frac{m_3}{m_1+m_2}\right)^{2/5} \frac{(1+e_2)^{2/5}}{(1-e_2)^{6/5}}\left(1-\frac{0.3i}{180}\right), \tag{3}$$

where m_1 and m_2 are the masses of the binary components,

m_3 is the mass of the tertiary and i is the inclination of the inner to outer orbit. The time scale on which KL operates at the lowest order can be found as (Antognini 2015):

$$t_{\rm KL} \sim \frac{16}{15} \frac{a_2^3 (1-e_2^2)^{3/2} \sqrt{m_1 + m2}}{a_1^{3/2} m_3 G}. \tag{4}$$

Furthermore, we verify that the timescale of the precession of the perihelion of the inner orbit due to General Relativity effects ($t_{\rm 1PN}$) is longer than the $t_{\rm EKL}$, to assures that the KL effect is not suppressed by GR precession. To the first Post Newtonian order the relation between these two timescales can be estimated as (Naoz 2016):

$$\frac{t_{\rm 1PN,inner}}{t_{\rm KL}} = \frac{a_1^4}{3a_2^3} \frac{(1-e_1^2) m_3 c^2}{(1-e_2^2)^{3/2} (m_1+m_2)^2 G^2}. \tag{5}$$

We mark the triples that verify this criterion with a red cross in Fig. 5.

At the current stage of the project more simulations are required to test:

(i) the timescale for EKL triples in our systems;
(ii) how likely the conditions for the EKL mechanism can occur in our simulations;
(iii) whether the properties of the triples in Fig. 5 depend on the inclination of the inner to outer binary, in order to understand if EKL triples have the same properties of the other triple systems; if this is the case the probability of EKL triples can be simply estimated as the probability to have a large i.

Once these tests are done, the merger rate in a PBH cluster will be approximately equal the EKL triple formation rate, and to a zero order can be estimated as

$$\Gamma \approx N_{\rm binaries} \times f_{\rm triples} \times f_{\rm EKL}, \tag{6}$$

where $N_{\rm binaries}$ is the number of binaries per DM halo, $f_{\rm triples}$ is the fraction of binaries in hierarchical triple systems and $f_{\rm EKL}$ is the fraction of triples that undergo the EKL mechanism and merge in less than a Hubble time. Finally, the total merger rate per unit volume can be obtained by multiplying Γ with the number of collapsed DM halos in the Universe per unit volume per unit mass $N(M)$. To compute $N(M)$ we adopt the Press-Schechter mass function (Press & Schechter 1974):

$$dN = \sqrt{\frac{\pi}{2}} \frac{d\sigma}{dM} \frac{\rho_{\rm m}^0 \delta_{\rm c}}{M\sigma^2} \exp\left(-\delta_{\rm c}^2/2\sigma_{\rm M}^2\right), \tag{7}$$

where $\delta_{\rm c} = 1.686$, $\rho_{\rm m}^0$ is the matter density at the present time and $\sigma_{\rm M}$ is the variance of linear perturbations of the mass scale M. In the regime of small mass halos $\delta_{\rm c}^2/2\sigma_{\rm M}^2 < 1$, we can neglect the exponential term and integrate the Press-Schechter mass function in the range of interest:

$$N = \sqrt{\frac{\pi}{2}} \rho_{\rm m}^0 \delta_{\rm c} \int_{M_{\rm min}}^{M_{\rm max}} \frac{d\sigma_{\rm M}}{dM} \frac{dM}{M\sigma_{\rm M}^2}. \tag{8}$$

The extremes of the integral can be found by considering the validity of the results obtained in our simulations. We will determine the parameter space describing PBH clusters in which the scenario described in Sect. 3 is valid. Ultimately, we will obtain the merger rate due to the EKL effect to compare with that from Bird et al. (2016).

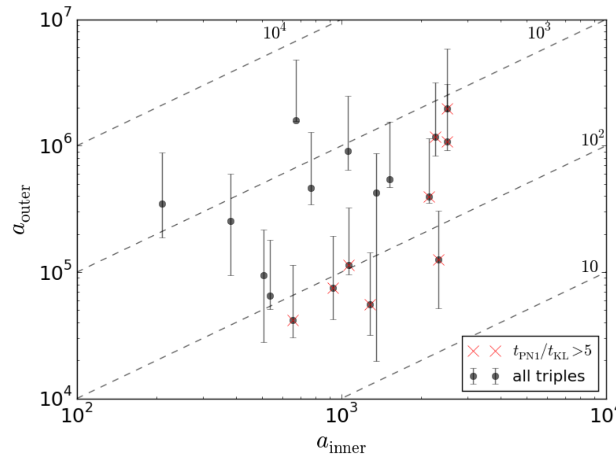

Figure 5. Properties of the triple systems formed in our simulations: circles represent the semi-major axis of the inner and outer binary respectively on the x and y-axis, the error bars on the y-axis represent $a_2(1-e_2)$ and $a_2(1+e_2)$, and dashed lines are the lines of the constant ratio $a_{\rm inner}/a_{\rm outher}$.

5 DISCUSSION AND CONCLUSIONS

Our results indicate that the estimates for the merger rate of binary BHs of primordial origin should be conducted more carefully in the regime of small mass DM halos. We show that few-body dynamical interactions in clusters of 10^3 M⊙ mass and 1 pc size lead to formation of hard binaries. We find that typically one or two hard binaries are formed in our simulations. Once a hard binary is formed, the cluster evaporates in $\sim 10-20$ crossing times. We expect that our results will reduce the merger rate of PBH binaries reported in the literature. More simulations are required to quantify this expectation.

ACKNOWLEDGEMENTS

We acknowledge the Kavli Foundation and the DNRF for supporting the 2017 Kavli Summer Program, and thank the Niels Bohr Institute for its hospitality while part of this work was completed. VK was supported by NWO WRAP Program, grant NWO 648.003004 APP-GW. Simulations in this paper made use of the REBOUND code which can be downloaded freely at http://github.com/hannorein/rebound.

References

Abbott B. P., et al., 2016, Phys. Rev. Lett., 116, 061102
Alcock C., et al., 2000, ApJ, 542, 281
Ali-Haïmoud Y., Kovetz E. D., Kamionkowski M., 2017, preprint, (arXiv:1709.06576)
Antognini J. M. O., 2015, MNRAS, 452, 3610
Bird S., Cholis I., Muñoz J. B., Ali-Haïmoud Y., Kamionkowski M., Kovetz E. D., Raccanelli A., Riess A. G., 2016, Physical Review Letters, 116, 201301
Carr B., Kühnel F., Sandstad M., 2016, Phys. Rev. D, 94, 083504
Cholis I., Kovetz E. D., Ali-Haïmoud Y., Bird S., Kamionkowski M., Muñoz J. B., Raccanelli A., 2016, Phys. Rev. D, 94, 084013
Clesse S., García-Bellido J., 2016, preprint, (arXiv:1610.08479)

Hawking S., 1971, MNRAS, 152, 75
Kozai Y., 1962, AJ, 67, 591
Lidov M. L., 1962, Planet. Space Sci., 9, 719
Mardling R. A., Aarseth S. J., 2001, MNRAS, 321, 398
Naoz S., 2016, ARA&A, 54, 441
Paczynski B., 1986, ApJ, 304, 1
Peters P. C., 1964, Physical Review, 136, 1224
Press W. H., Schechter P., 1974, ApJ, 187, 425
Quinn D. P., Wilkinson M. I., Irwin M. J., Marshall J., Koch A., Belokurov V., 2009, MNRAS, 396, L11
Rein H., Liu S.-F., 2012, A&A, 537, A128
Rein H., Spiegel D. S., 2015, MNRAS, 446, 1424
Sasaki M., Suyama T., Tanaka T., Yokoyama S., 2016, Physical Review Letters, 117, 061101
Tisserand P., et al., 2007, A&A, 469, 387
Yoo J., Chanamé J., Gould A., 2004, ApJ, 601, 311